

Inhibition of DNA-PK activity sensitizes A549 cells to X-ray irradiation by inducing the ATM-dependent DNA damage response

LINA YANG¹, XINRUI YANG², YIWEI TANG¹, DEFU ZHANG¹, LIJIE ZHU¹,
SHENGNAN WANG¹, BO WANG¹ and TAO MA¹

¹College of Food Science and Technology, Bohai University, Jinzhou, Liaoning 121013;

²Center for Therapeutic Research of Hepatocarcinoma, Beijing 302 Hospital, Beijing 100039, P.R. China

Received October 6, 2017; Accepted February 16, 2018

DOI: 10.3892/mmr.2018.8828

Abstract. Non-small cell lung cancer (NSCLC) is radioresistant to X-rays due to powerful cellular DNA damage repair mechanisms. DNA-dependent protein kinase (DNA-PK) is a key enzyme involved in DNA damage repair and the phenomenon and molecular mechanism of NSCLC radiosensitivity were investigated following inhibition of DNA-PK activity. In the present study A549 cells were treated with the DNA-PK inhibitor NU7026 and/or siRNA directed against ataxia telangiectasia mutated (ATM), followed by exposure to 4 Gy X-ray irradiation. Radiosensitivity, DNA damage, apoptosis and protein expression were measured by colony formation assay, γ H2AX foci immunofluorescence, Annexin V/PI staining and western blotting, respectively. A Balb/c-nu/nu xenograft mouse model was established by subcutaneous injection of A549 cells and was used to examine the effect of administering NU7026 via intraperitoneal injection prior to 4 Gy X-ray exposure. The xenograft tumors were weighed and observed by hematoxylin and eosin staining after irradiation. NU7026 treatment followed by X-ray irradiation significantly decreased the colony formation ratio of A549 cells, and increased γ H2AX foci and cell apoptosis. Furthermore, the combined treatment of NU7026 and X-rays resulted in growth inhibition and cell apoptosis in A549 xenograft tumors. Consequently, apoptosis regulators full-length transactivating (TA) p73 and an N-terminally truncated (DN) p73 were upregulated and downregulated respectively, leading to activation of glucosyltransferases and Rab-like GTPase activators and myotubularins domain-containing 4 (GRAMD4) protein to reduce the Bcl-2/Bax protein ratio.

In addition, ATM siRNA efficiently prevented γ H2AX foci formation, and enhanced NU7026-induced inhibition of survival and promoted apoptosis. In conclusion, inhibition of DNA-PK activity increased the radiosensitivity of A549 cells to X-ray irradiation. NU7026 treatment activated the ATM-dependent DNA damage response and induced p73 apoptosis pathway. DNA-PK inhibitor may be an effective constituent of radiosensitization products. DNA damage repair pathway could be a potential target for radiosensitization.

Introduction

Lung cancer is a leading cause of cancer mortality, accounting for over 1 million deaths per year worldwide (1,2). Lung cancer has been classified into small-cell lung cancer and non-small cell lung cancer (NSCLC) according to their histological types (1). NSCLC accounts for at least 85% of all lung cancers, with increasing incidence and mortality in developing countries (2). Radiotherapy is a common method used in NSCLC clinical treatment, including X-rays and γ -rays, which provide low-linear energy transfer. However, NSCLC cells demonstrate poor response to radiotherapy due to radioresistance (3). The radiosensitivity of NSCLC cells is therefore one of the most important factors for improving the curative effect of radiotherapy.

Powerful DNA damage repair systems in cancer cells contribute to radioresistance, including the non-homologous end joining (NHEJ) and the homologous recombination (HR) pathways (4). The HR repair pathway only occurs in the S and G₂ phases of the cell cycle, while the NHEJ pathway can occur in all the cell cycle phases (5). Notably, DNA repair kinetics of the NHEJ pathway are much faster than those of the HR repair pathway (6,7). Therefore, NHEJ is the dominant DNA damage repair pathway in mammalian cells. Previous studies have identified members of the phosphoinositide-3 kinase family that participate in the NHEJ and HR pathways, including DNA-dependent protein kinase (DNA-PK) and ataxia telangiectasia mutated (ATM), respectively (4,8). It has been hypothesized that inhibition of DNA-PK activity can block the NHEJ process to increase radiosensitivity (9,10).

Correspondence to: Professor Tao Ma, College of Food Science and Technology, Bohai University, 19 Keji Road, Songshan New Region, Jinzhou, Liaoning 121013, P.R. China
E-mail: matao-09@163.com

Key words: A549, DNA-PK, radiosensitivity, xenograft tumor, X-rays

Cell apoptosis is another significant factor in the process of blocking DNA damage repair pathways and is regulated by a complex balance in signaling pathways controlling pro- and anti-apoptotic factors (11). p73 serves a key role in apoptosis induction, encoding two types of protein isoform: Full-length transactivating (TA) p73 and an N-terminally truncated (DN) p73 (12,13). TAp73 can activate the transcription of cell cycle and apoptosis regulators, thus acting as a pro-apoptotic factor (14), while DNp73 is able to bind to DNA and form dimers with TAp73 as a dominant negative anti-apoptotic factor (12,15). Overexpression of DNp73 and the low expression of TAp73 have frequently been detected in radioresistant cancer cells (e.g., cervical cancer, breast cancer and non-Hodgkin lymphoma), leading to activated mitochondrial effector protein glucosyltransferases and Rab-like GTPase activators and myotubularins domain-containing 4 (GRAMD4) to reduce the Bcl-2/Bax ratio in mitochondria (16-18). This suggested that increasing TAp73 and/or decreasing DNp73 may enhance the radiosensitivity of NSCLC cells.

NU7026 (2-(4-Morpholinyl)-4H-naphtho[1,2-b]pyran-4-one) is a novel DNA-PK inhibitor, which has been studied for the treatment of human immunodeficiency virus and leukemia (19). In the present study, NU7026 was used to reduce the DNA damage repair capacity and its effect on the radiosensitivity of A549 lung cancer cells and xenograft tumors was investigated. The present results may be useful in assessing the clinical potential of NU7026 and may also identify the molecular mechanisms involved in the regulation of the DNA damage response and cell apoptosis. The present study may therefore serve as an important supplement to our knowledge regarding the underlying mechanisms of radiosensitivity.

Materials and methods

Cell culture and RNA interference. A549 lung cancer cells were purchased from ATCC and cultured in Dulbecco's modified Eagle's medium (DMEM; Invitrogen; Thermo Fisher Scientific, Inc., Waltham, MA, USA) supplemented with 10% fetal bovine serum (FBS; Hyclone; GE Healthcare, Chicago, IL, USA). The cells were incubated in 95% humidified atmosphere at 37°C in the presence of 5% CO₂ to maintain exponential cell growth. A549 cells were plated in 60 mm dishes at a concentration of 2.0×10^5 cells. On the second day, 100 nM SignalSilence® ATM siRNA I (Cell Signaling Technology, Inc., Danvers, MA, USA) targeting the ATM (5'-CUAACAACAGGUGAUUAU-3') was mixed with Lipofectamine® 2000 in serum-free DMEM medium transfected A549 cells. The transfection controls included 100 nM scramble siRNA (5'-UGUUAUCAAAC AUGCAAUAG-3'; Takara Biotechnology Co., Ltd., Dalian, China) to exclude the effect of non-specific factors and treatment with Lipofectamine® 2000 alone to exclude the effect of the transfection reagent and untransfected controls (Cell Signaling Technology, Inc.).

DNA-PK inhibitor and irradiation treatment. DNA-PK inhibitor NU7026 (Abcam, Cambridge, UK) was dissolved in DMSO. $1-10 \times 10^6$ A549 cells were treated with 10 μ M NU7026 for 30 min, prior to being exposed to 4 Gy X-rays for 3.6 min at room temperature. NU7026 was not washed until the

sample was collected. All the treatments with NU7026 were performed in the same manner. X-rays were obtained from a Faxitron 43885D X-ray machine at 100 kVp energy. The X-ray dose was 1.1 Gy/min. Non-irradiated A549 cells were handled in parallel with the irradiated cells.

Colony formation assay. A549 cells (2×10^3 cells) were seeded in a 25-cm² culture flask with 0, 2, 4, 6 and 8 Gy X-ray irradiation. Similarly, A549 cells were treated with 10 μ M NU7026 for 30 min followed by 4 Gy X-ray irradiation. The cells were washed with phosphate-buffered saline (PBS), fixed with 70% ethanol and stained with Giemsa for 5 min at room temperature 10 days later. Colonies containing >50 cells were identified as survivors under a stereomicroscope. Survival fraction (SF2; 2 Gy) was calculated according to colonies.

Apoptosis analysis by Annexin V/PI staining. Apoptosis was measured using the Annexin V-FITC Apoptosis Detection kit (Bestbio, Shanghai, China). Briefly, approximately 1×10^6 cells per experimental condition (Control, NU7026, 4 Gy, NU7026+4 Gy, ATM siRNA, ATM siRNA+NU7026, ATM siRNA+4 Gy and ATM siRNA+NU7026+4 Gy) were collected after trypsinisation at 24 h post-irradiation, washed with cold PBS twice, and resuspended with 400 μ l binding buffer. After adding 5 μ l of Annexin V-FITC solution and 10 μ l PI (Abcam) solution, the cells were incubated for 15 min at room temperature in the dark. After the incubation, 10,000 cells were analyzed with the FACSCalibur flow cytometer (BD Bioscience, Franklin Lakes, NJ, USA) and FlowJo version 7.6 software (FlowJo LLC, Ashland, OR, USA).

γ H2AX foci immunofluorescence. The cells were seeded in a 6-well plate at a density of 1×10^5 cells/well. The cells per experimental condition were treated with 10 μ M NU7026 for 30 min, prior to being subjected to 4 Gy X-ray irradiation. At 30 min post-irradiation, the A549 cells were fixed with 4% paraformaldehyde for 15 min, and then treated with 0.1% Triton X-100 for 30 min and 5% BSA for 1 h at room temperature. Subsequently, the cells were incubated with primary monoclonal antibody anti- γ H2AX (cat. no. 9718; 1:500; Cell Signaling Technology Inc.) at room temperature for 2 h. Subsequently, the cells were incubated at room temperature for 1 h with IgG-fluorescein isothiocyanate (cat. no. A0562; 1:500; Bestbio) in the presence of 1% BSA. Following the addition of 20 μ l DAPI (1.5 μ g/ml) to counterstain the nuclei, γ H2AX foci were detected with a confocal microscope. When the sizes of γ H2AX foci were $>0.01 \mu\text{m}^2$, the number of γ H2AX foci was counted in three random fields.

Western blot analysis. A total of $1-10 \times 10^6$ cells were treated with NU7026 for 30 min at room temperature prior to 4 Gy X-ray irradiation. At 24 h post-irradiation, A549 cells were lysed in 0.5 ml RIPA lysis buffer (Bestbio) supplemented with 1 mM PMSF (Sigma-Aldrich; Merck KGaA, Darmstadt, Germany) for 1 h on ice, and protein concentration was detected by BCA kit (Beyotime Institute of Biotechnology). The protein was separated on sodium dodecyl sulfate polyacrylamide gel electrophoresis (SDS-PAGE) with 10% separating gel and 4% stacking

gel (Bioworld Technology, Inc., St. Louis, MN, USA) at 80 V for 2 h and transferred to polyvinylidene difluoride membranes (Bio-Rad Laboratories, Inc., Hercules, CA, USA) for 2 h at room temperature. The membranes were blocked for 1 h with PBS containing 5% BSA, and incubated with the corresponding primary monoclonal antibody IgG anti-TAp73 (cat. no. 5B429; 1:1,000; Novus Biologicals, Littleton, CO, USA), DNp73 (cat. no. 38C674.2; 1:1,000; Novus Biologicals), GRAMD4 (cat. no. sc-515128; 1:1,000; Santa Cruz Biotechnology, Dallas, TX, USA) and p53 (cat. no. 9282; 1:1,000), Bcl-2 (cat. no. 2872; 1:1,000), Bax (cat. no. 2772; 1:1,000), γ H2AX (cat. no. 9718; 1:1,000), ATM (cat. no. 2873; 1:1,000), DNA-PK (cat. no. 4620; 1:1,000) and β -actin (cat. no. 4970; 1:1,000; all Cell Signaling Technology Inc.) at 4°C overnight. Subsequently, the membranes were washed with PBS with Tween for 30 min at room temperature, incubated with an HRP-conjugated goat anti-rabbit or goat anti-mouse secondary antibody (1:5,000; Cell Signaling Technology, Inc., Dallas, TX, USA) for 1 h at room temperature. Following 3 washes with PBS with Tween-20 for 10 min at room temperature, a chemiluminescence kit (Santa Cruz Biotechnology, Inc.) was used to detect proteins. The intensity of protein was measured by AlphaView software (version 3.4.0.0729; ProteinSimple, San Jose, CA, USA).

Nude mouse xenograft model. A total of 20, seven-week-old male nude mice (Balb/c-nu/nu) were purchased from the Institute of Laboratory Animal Sciences, Institute of Laboratory Animal Sciences (Beijing, China). The mice were housed at the animal research facility under pathogen-free conditions in 40-60% humidified atmosphere at 26-28°C for 10 h light and 14 h dark cycle. Mice were randomly allocated into control, NU7026, 4 Gy and NU7026+4 Gy groups with 5 animals per group and provided with standard laboratory food and tap water *ad libitum*. Exponentially growing A549 cells (2×10^7 cells in 100 μ l) were injected subcutaneously into the backs of the mice and tumors were visible on the 7th day. Little adverse reactions were observed during the tumor formation. Tumor growth was evaluated every two days by measurement of the tumor major (a) and minor (b) axes, from which the tumor volume (V) was calculated according to the formula: $V = ab^2/2$. When tumors became 10 mm in diameter and 250-300 mm³ in volume, NU7026 (25 mg/kg, 200 μ l) was administered via intraperitoneal injection into tumor-bearing mice in the treatment group for 30 min, prior to exposure to 4 Gy X-rays. Other mice only received no-treatment, NU7026 treatment and 4 Gy irradiation, respectively. Mice were sacrificed by cervical dislocation under 3% aether after radiation treatment (day 15). The xenograft tumors were removed through-dissection and weighting. No animals were lost as a result of treatment or tumor progression. The study protocol was approved by the ethics committee of the Bohai University.

Hematoxylin and eosin (H&E) staining. One centimeter diameter tumors were fixed in 4% paraformaldehyde solution for 12 h at room temperature and embedded in paraffin. After cutting the paraffin into 5 μ m sections, the slides were dewaxed, rehydrated, and stained with 1% H&E at room temperature as described previously (20).

Statistical analysis. Data are presented as the mean \pm standard deviation from ≥ 3 independent experiments. Several independent samples were evaluated for statistical significance with one-way analysis of variance followed by Turkey's test, using SPSS 11.0 software (SPSS, Inc., Chicago, IL, USA). $P < 0.05$ was considered to indicate a statistically significant difference.

Results

Inhibition of DNA-PK sensitizes A549 cells to X-ray irradiation.

Fig. 1 shows that the survival fractions of cells treated with 0, 2, 4, 6 and 8 Gy for 10 days were 1.00, 0.85, 0.47, 0.15 and 0.06, respectively (Fig. 1A). The expression of DNA-PK was inhibited in the NU7026 or NU7026+4 Gy groups, but DNA-PK increased in the 4 Gy group (Fig. 1B). The expression of ATM was almost unchanged in the four groups after NU7026 treatment (Fig. 1B). The survival fraction of A549 cells after NU7026+4 Gy treatment was a 79.3% decrease relative to 4 Gy X-ray irradiation alone ($P < 0.001$). Moreover, no statistically significant difference was evident between control and NU7026-treated cells ($P > 0.05$; Fig. 1C). NU7026 increased the sensitivity of A549 cells to X rays by 4.8-fold.

Inhibition of DNA-PK and X-ray irradiation increases DNA damage and cell apoptosis. γ H2AX foci are biomarkers of DNA double-strand breaks that initiate the DNA damage response (21). In the present study, X-ray irradiation significantly increased γ H2AX foci (Fig. 1D). The greatest number of γ H2AX foci was observed after NU7026 and 4 Gy X-ray co-treatment, followed by the 4 Gy irradiation-alone group. NU7026 treatment and/or X-ray irradiation significantly increased late apoptosis (Fig. 1E). The late apoptosis rate in the control group was $4.58 \pm 0.2\%$ and increased to 5.9 ± 0.7 , 9.7 ± 0.5 and $82.5 \pm 2.6\%$ in the NU7026, 4 Gy and NU7026+4 Gy groups, respectively (Fig. 1E).

Inhibition of DNA-PK and X-ray irradiation induces p73 apoptosis pathway in A549 cells. The expression of cell apoptosis regulatory proteins was analyzed by western blot analysis and the results are shown in Fig. 2. At 24 h post-irradiation, NU7026 pre-treatment decreased DNp73 expression and increased p53 and TAp73 expression at the protein level. Downstream GRAMD4 was also upregulated. Furthermore, anti-apoptotic factor Bcl-2 expression was downregulated and pro-apoptotic factor Bax expression was upregulated.

Inhibition of DNA-PK sensitizes xenograft tumors to X-ray irradiation. Xenograft tumor growth was recorded 15 days post-irradiation (Fig. 3A). Little adverse reactions of all mice were observed during tumor formation. But with the increase of the tumor volume in the control and the NU7026 treatment groups, the activity of nude mice decreased, the mental state was poor with drowsiness and less exercise, and the weight loss (6.5 ± 1.3 and 5.8 ± 1.1 g, respectively). The adverse reactions of nude mice in X-ray and NU7026+X-rays treatment groups were not present. The results indicated that each nude mouse is loaded with one tumor. The tumor growth was not restricted in the control group, where the mean tumor weight was 0.76 ± 0.03 g (longest diameter = 19.19 ± 3.27 mm, volume = $1,401.24 \pm 32.32$ mm³), nor was tumor growth

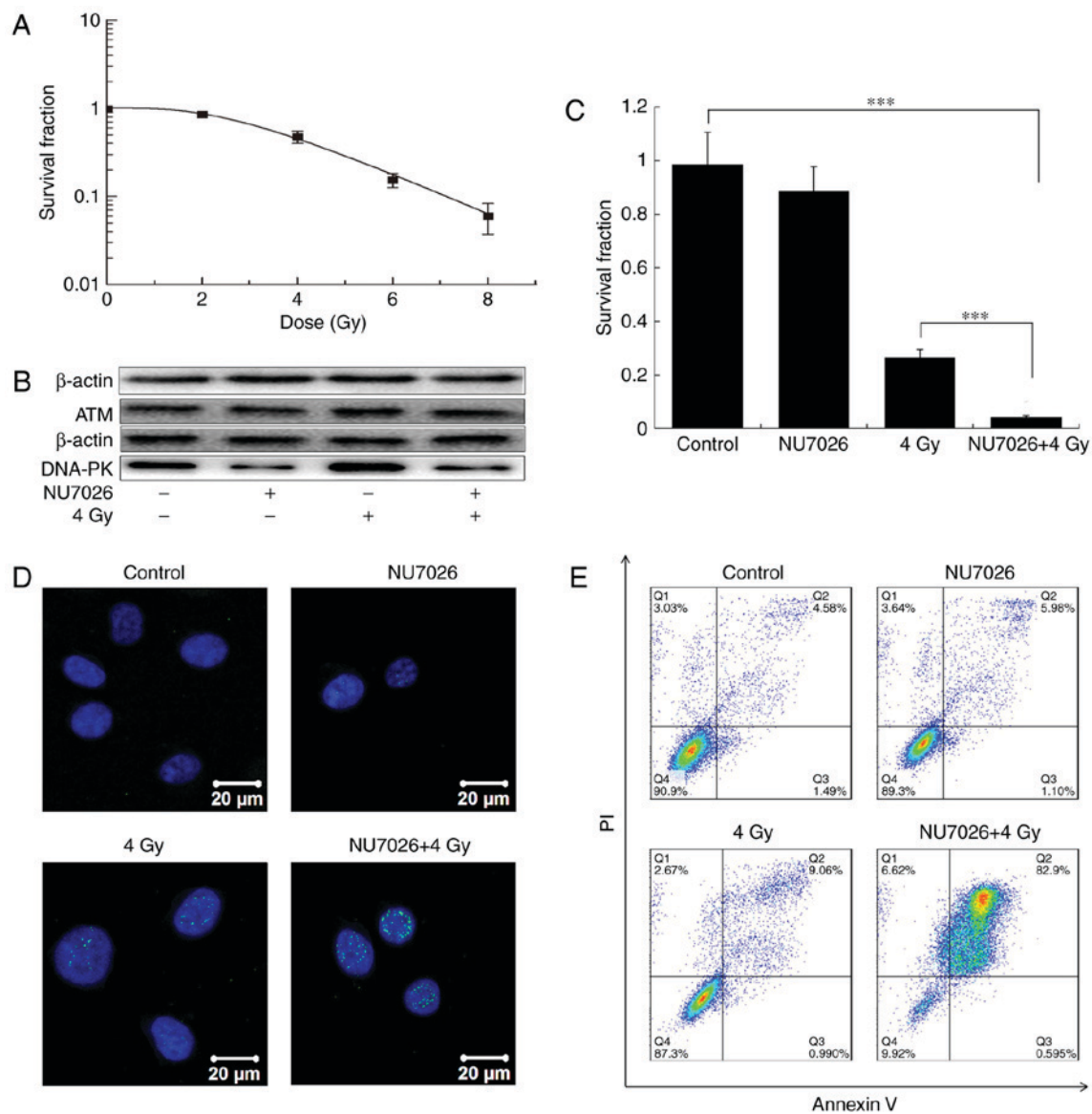


Figure 1. Effects of NU7026 and X-rays on growth, DNA damage and apoptosis in A549 cells. (A) The survival fraction was calculated after 0, 2, 4, 6 and 8 Gy X-ray irradiation. (B) Protein levels of DNA-PK and ATM were determined by western blotting 24 h post-treatment, following treatment with no-irradiation, 10 μ M NU7026, 4 Gy X-rays and 10 μ M NU7026+4 Gy X-rays. (C) The survival fraction was calculated after 10 μ M NU7026 and 4 Gy X-ray irradiation. *** P <0.001. (D) γ H2AX foci were imaged and detected by immunofluorescence 0.5 h post-irradiation. (E) Apoptosis was analyzed by flow cytometry after Annexin V/PI staining 24 h post-irradiation.

significantly inhibited in the NU7026 treatment group with a mean tumor weight of 0.71 ± 0.07 g (longest diameter = 14.78 ± 4.65 mm, volume = $1,205.75 \pm 82.55$ mm³; Fig. 3B and C). In contrast, tumor growth was significantly inhibited in the X-ray and NU7026+X-rays treatment groups with mean tumor weights of 0.61 ± 0.18 g (longest diameter = 13.27 ± 3.02 mm, volume = 930.13 ± 32.86 mm³) and 0.42 ± 0.15 g (longest diameter = 9.24 ± 2.10 mm, volume = 308.38 ± 12.39 mm³), respectively (P <0.001; Fig. 3B and C). The tumor weight of NU7026+4 Gy was a 31.1% decrease compared with 4 Gy X-ray irradiation alone (P <0.001). NU7026 increased the sensitivity of tumors to X rays by 1.5 times. The effects of NU7026+X-ray irradiation treatment was also examined by H&E staining. The results indicated that necrosis of tumor tissue gradually increased, especially in the NU7026+X-ray irradiation group with increased cytoplasm (pink; Fig. 3D) and fragmented nuclei (arrows; Fig. 3E).

ATM gene silencing promotes NU7026/X-ray-induced inhibition of survival and apoptosis. In ATM siRNA-transfected cells, NU7026 and/or X-ray treatment decreased survival fraction (Fig. 4). The survival fraction of A549 cells after ATM siRNA+NU7026+X-ray treatment decreased by 94.1% compared with ATM siRNA treatment (P <0.001), and decreased by 35.2% compared with ATM siRNA+X-ray treatment (P <0.001; Fig. 4A). Late apoptosis in ATM siRNA-transfected cells was significantly increased by NU7026 treatment and/or X-ray treatment. The late apoptosis rate of the ATM siRNA treatment group was $4.84 \pm 0.5\%$ compared with $6.3 \pm 0.4\%$ in the ATM siRNA+NU7026 group, $10.8 \pm 1.6\%$ in the ATM siRNA+X-rays group and $84.2 \pm 1.9\%$ in the ATM siRNA+NU7026+X-rays group (Fig. 4B). These results demonstrated that ATM gene silencing enhanced the inhibition of survival and promoted apoptosis induced by NU7026/X-ray treatment.

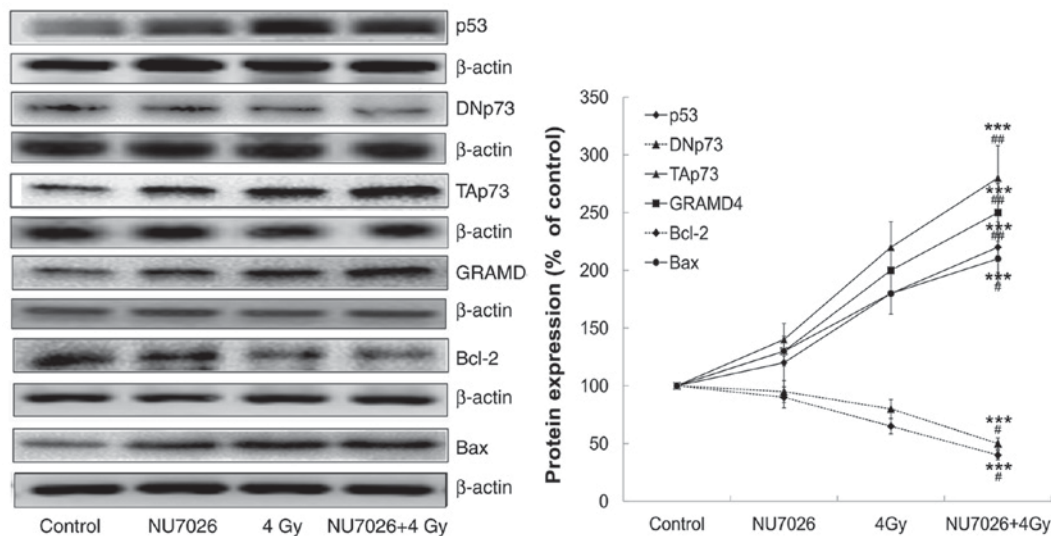


Figure 2. Effects of NU7026 and X-rays on expression of apoptosis-related proteins in A549 cells. The protein levels of p53, DNp73, TAp73, GRAMD4, Bcl-2 and Bax were determined by western blotting 24 h post-irradiation, following treatment with 10 μ M NU7026 for 30 min and 4 Gy X-rays. *** P <0.001 vs. the control group, # P <0.05 and ## P <0.01 vs. the 4 Gy group.

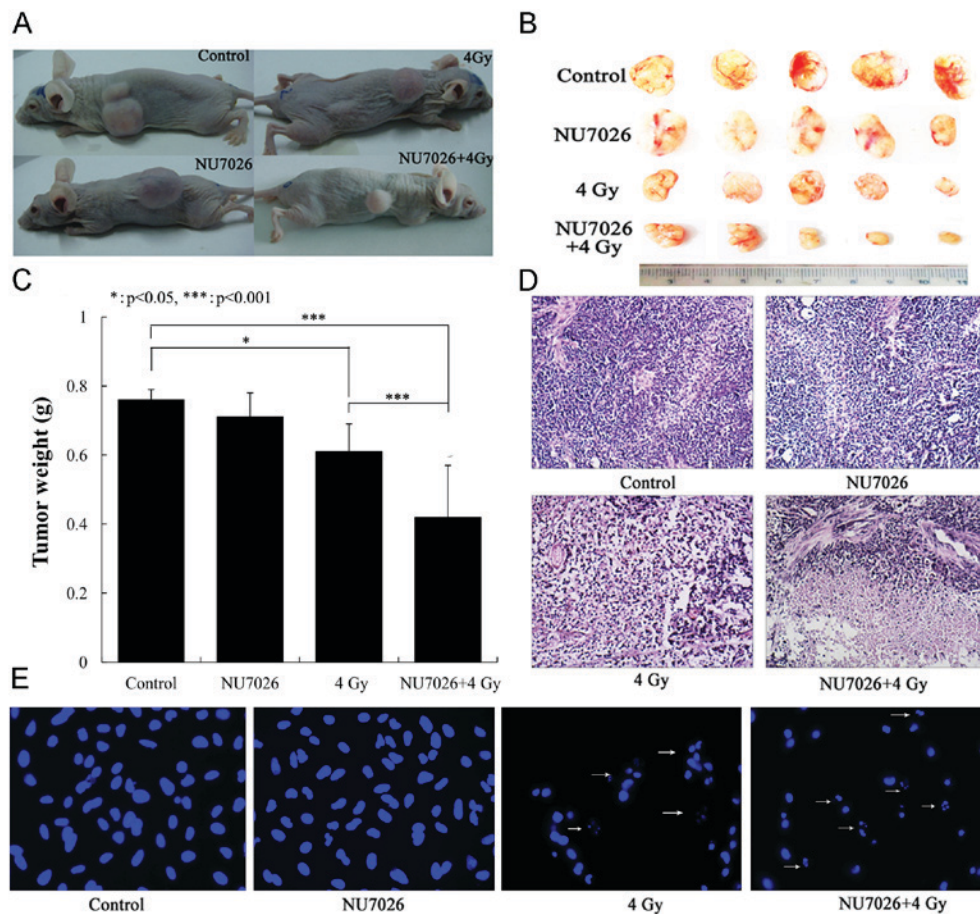


Figure 3. Effects of NU7026 combined with X-ray irradiation on tumor growth in an A549 xenograft model 15 days post-irradiation. (A) Xenograft mice were imaged, following pre-treatment with 10 μ M NU7026 for 30 min via intraperitoneal injection. Tumors were excised (B) and weighed (C) at the end of the experiment. * P <0.05 and *** P <0.001. (D) H&E staining of tumor tissues from different groups (magnification, x400). (E) DAPI staining of the nucleus of tumor tissue were detected with a confocal microscope. Arrows represent nuclear fragmentation.

ATM gene silencing reduces the NU7026+X-ray-induced DNA damage response. The number of γ H2AX foci was increased by ATM siRNA+4 Gy treatment compared with

the ATM siRNA and ATM siRNA+NU7026 groups. In contrast, the number of γ H2AX foci was decreased after ATM siRNA+NU7026+4 Gy treatment (Fig. 4C). These results

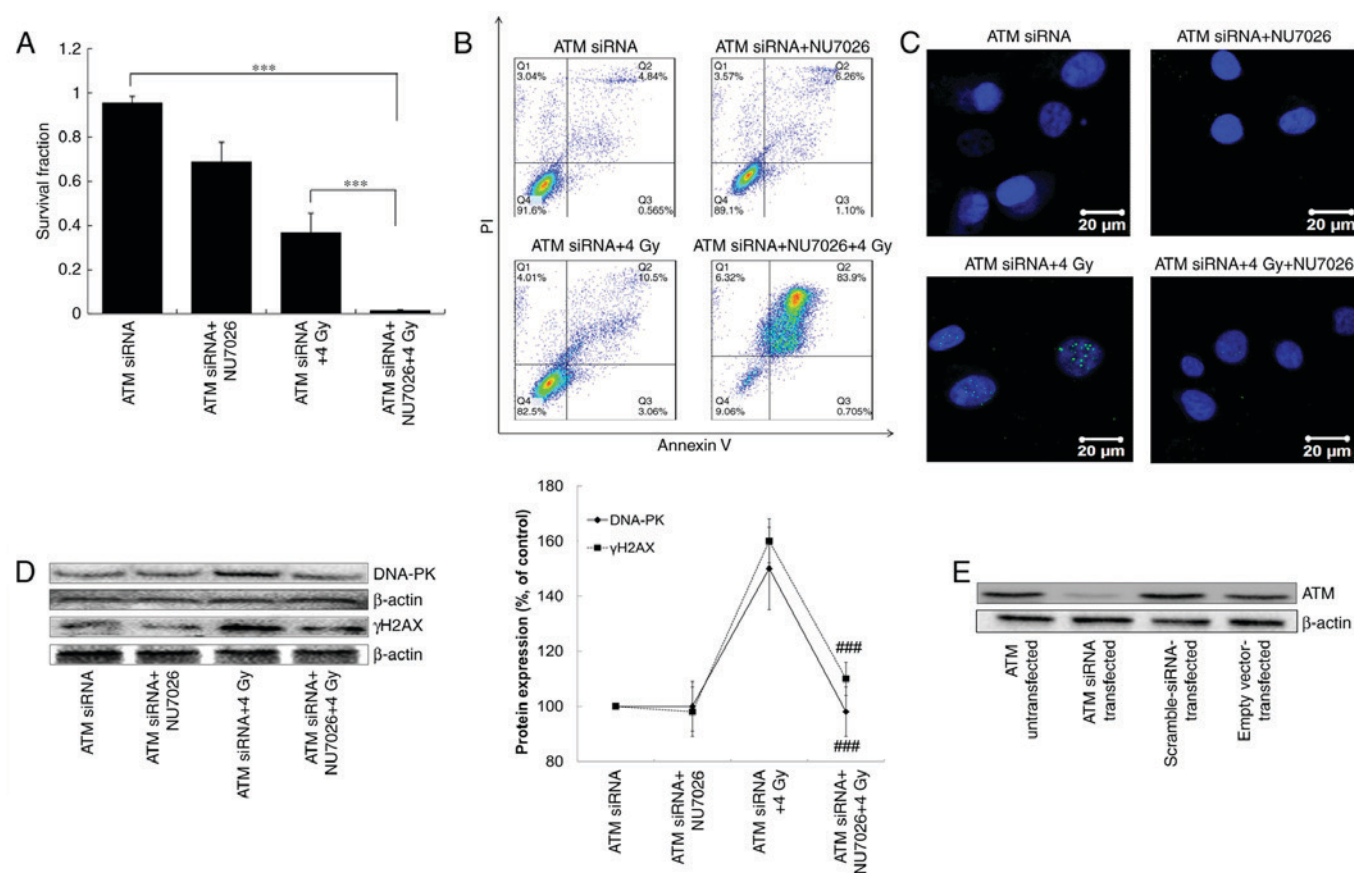


Figure 4. Effects of NU7026 and X-rays on growth, apoptosis and DNA damage in ATM siRNA-transfected A549 cells 24 h post-irradiation. (A) Survival fraction was calculated. *** $P < 0.001$. (B) Apoptosis was analyzed by Annexin V/PI staining. (C) γ H2AX foci were imaged and detected by immunofluorescence. (D) Expression of DNA-PK and γ H2AX protein was determined by western blotting. ### $P < 0.001$ vs. the ATM siRNA+4 Gy group. (E) The expression of ATM protein has been detected by western blotting in the transfected A549 cells.

paralleled γ H2AX protein expression in the same groups (Fig. 4D). However, the expression of DNA-PK was almost unchanged in ATM siRNA, ATM siRNA+NU7026 and ATM siRNA+NU7026+4 Gy groups. These results indicated that γ H2AX foci disappeared after NU7026+4 Gy treatment in ATM siRNA-transfected A549 cells compared with normal cells. Therefore, ATM but not DNA-PK, was involved in the NU7026+X-ray-induced DNA damage response. When the ATM-mediated repair pathway was inhibited, cells initiated programmed cell death. The desired effects of ATM-siRNA transfection have been achieved, that is, the expression of ATM protein has been reduced by western blotting in the transfected A549 cells (Fig. 4E).

Discussion

NSCLC has a strong capacity to repair DNA damage, which is the main reason for cancer radioresistance. DNA-PK serves an important role in NHEJ DNA damage repair (4,8). NU7026 (DNA-PK inhibitor) has been demonstrated to enhance the antitumor effect of X-rays against lung adenocarcinoma (10). The results of the current study revealed that NU7026 significantly increased the radiosensitivity of NSCLC cells exposed to X-ray irradiation by inhibiting the growth of A549 cells and xenograft tumors. The inhibitor

NU7026 may therefore be useful as a radiosensitizing drug for radiotherapy.

The sampling times of γ H2AX protein for confocal microscopy and other proteins for western blotting were 30 min and 24 h post-irradiation, respectively. Usually DNA damage occurs within 30 min post-irradiation. Subsequently, cells activate the DNA damage response pathway >30 min (5,6). DNA damage agents can also activate the DNA damage response pathway, which either results in DNA repair or apoptosis of cancer cells (22-25). In the present study, the radiosensitizing effects of NU7026 on NSCLC cells were further investigated. The results demonstrated that inhibition of DNA-PK increased DNA damage and initiated the ATM-dependent DNA damage response after X-ray irradiation. It was also illustrated that NU7026 pre-treatment activated apoptosis of NSCLC cells, indicating that inhibition of DNA-PK could result in persistent DNA damage. ATM is involved in activation of the downstream p73 apoptotic pathway when DNA damage repair fails (14). Overexpression of the TAp73 isoform directly activated pro-apoptotic factor GRAMD4 expression to induce changes in Bcl-2 and Bax protein levels in mitochondria. Decreased Bcl-2/Bax ratio contributes to apoptosis (11). In addition, our previous study demonstrated that ATM knock-down effectively inhibited cell growth and increased DNA damage and apoptosis in NSCLC cells after co-treatment with NU7026 and X-ray irradiation (10). Therefore, combining

the ATM specific inhibitor CGK733 and DNA-PK inhibitor NU7026 may more effectively block DNA damage repair and enhance radiosensitivity of NSCLC cells.

Previous studies have demonstrated that DNA-PK inhibitors can enhance the radiosensitivity of cancer cells (liver cancer HepG2, gastric cancer N87 and leukaemia MOLT-4) by increasing DNA damage leading to G₂/M phase arrest and induction of apoptosis (22-28). Similarly, the present results demonstrated that a DNA-PK inhibitor exerted radiosensitization effects on xenograft tumors *in vivo* and on A549 cells *in vitro*. John *et al* (13) demonstrated that p73 was able to trigger apoptosis via the mitochondrial pathway by the newly discovered pro-apoptotic mediator GRAMD4 (death-inducing protein), which induced changes in Bcl-2 and Bax protein expression.

A recent study has revealed that ATM-dependent DNA repair response of cervical cancer cells were activated by 7-hydroxy-5,4'-dimethoxy-2-arylbenzofuran via causing DNA damage as an anti-cancer agent (29). Moreover, several cancer cell lines that lack ATM function have enhanced sensitivity to radiotherapy and chemotherapy (10,30,31). The function of DNA-PK and ATM is complementary since it has been demonstrated that combined knockout of both kinases is synthetically lethal (32). Therefore, it could be proposed that inhibition of DNA-PK activates the ATM-dependent DNA damage response and that ATM knockdown increases the radiosensitivity of NSCLC cells following X-ray irradiation.

DNA damage is a universal characteristic following cancer cell radiotherapy. Therefore, the use of DNA repair inhibitors alone or in combination may have great radiosensitizing potential (10,33-37). The key factors in the DNA damage repair pathway include PARP, ATM, ATR, DNA-PK, Chk1 and Chk2, among others (33-39). PARP inhibitors have been demonstrated to interfere with single strand break (SSB) repair in HR-defective cancer cells at a safe dose level in combination with chemotherapy and radiotherapy in clinical trials (33). ATM and ATR inhibitors (caffeine and KU-55933, respectively) induce phosphorylation of p53 to promote radiosensitization, but low serum levels and high systemic toxicity have been limiting factors in clinical trials (34). DNA-PK inhibitors wortmannin and LY294002 are neither specific nor suitable for clinical use due to severe toxicity (35,36). The pharmacokinetics of NU7026 and NU7441 (another DNA-PK inhibitor) are still undergoing clinical analysis (37). Chk1 inhibitors (UCN-01) have demonstrated a long half-life and decreased bioavailability, whereas the Chk1 and Chk2 inhibitor PF-00477736 resulted in greater inhibition of tumor growth (38,39). Notably, the clinical development of inhibitors for PARP, ATM, ATR, Chk1, Chk2 and DNA-PK is being actively pursued (9). In summary, inhibition of DNA-PK activity enhanced the radiosensitivity of NSCLC cells to X-ray radiation by inducing the ATM-dependent DNA damage response and p73 apoptosis pathway, thus elucidating mechanisms underlying the myriad effects of DNA-PK, ATM, p73 and radiotherapy.

Acknowledgements

Not applicable.

Funding

The present study was funded by the National Natural Science Foundation of China (grant no. 31601510) and the Natural Science Foundation of Liaoning Province of China (grant no. 20170540022).

Availability of data and materials

The analyzed data sets generated during the study are available from the corresponding author on reasonable request.

Author's contributions

LY was a major contributor in study design, cell tests, data analysis and writing of the manuscript. TM also was a major contributor in study design. XY performed mice experiments. DZ and LZ analyzed and interpreted the data. YT, SW and BW performed cell tests. All authors read and approved the final manuscript.

Ethics approval and consent to participate

The study protocol was approved by the ethics committee of the Bohai University.

Consent for publication

Not applicable.

Competing interests

The authors declare that they have no competing interests.

References

1. Rodin D, Grover S, Xu MJ, Hanna TP, Olson R, Schreiner LJ, Munshi A, Mornex F, Palma D and Gaspar LE: International Association for the Study of Lung Cancer Advanced Radiation Technology Committee: Radiotherapeutic management of non-small cell lung cancer in the minimal resource setting. *J Thorac Oncol* 11: 21-29, 2016.
2. DeSantis CE, Lin CC, Mariotto AB, Siegel RL, Stein KD, Kramer JL, Alteri R, Robbins AS and Jemal A: Cancer treatment and survivorship statistics, 2014. *CA Cancer J Clin* 64: 252-271, 2014.
3. Yang HJ, Kim N, Seong KM, Youn H and Youn B: Investigation of radiation-induced transcriptome profile of radioresistant non-small cell lung cancer A549 cells using RNA-seq. *PLoS One* 8: e59319, 2013.
4. Zhuang W, Li B, Long L, Chen L, Huang Q and Liang Z: Induction of autophagy promotes differentiation of glioma-initiating cells and their radiosensitivity. *Int J Cancer* 129: 2720-2731, 2011.
5. Kim JS, Krasieva TB, Kurumizaka H, Chen DJ, Taylor AM and Yokomori K: Independent and sequential recruitment of NHEJ and HR factors to DNA damage sites in mammalian cells. *J Cell Biol* 170: 341-347, 2005.
6. Mahaney BL, Meek K and Lees-Miller SP: Repair of ionizing radiation-induced DNA double-strand breaks by non-homologous end-joining. *Biochem J* 417: 639-650, 2009.
7. Lieber MR: The mechanism of human nonhomologous DNA end joining. *J Biol Chem* 283: 1-5, 2008.
8. Yajima H, Lee KJ, Zhang S, Kobayashi J and Chen BP: DNA double-strand break formation upon UV-induced replication stress activates ATM and DNA-PKcs kinases. *J Mol Biol* 385: 800-810, 2009.

9. Yang SH, Kuo TC, Wu H, Guo JC, Hsu C, Hsu CH, Tien YW, Yeh KH, Cheng AL and Kuo SH: Perspectives on the combination of radiotherapy and targeted therapy with DNA repair inhibitors in the treatment of pancreatic cancer. *World J Gastroenterol* 22: 7275-7288, 2016.
10. Yang L, Liu Y, Sun C, Yang X, Yang Z, Ran J, Zhang Q, Zhang H, Wang X and Wang X: Inhibition of DNA-PKcs enhances radiosensitivity and increases the levels of ATM and ATR in NSCLC cells exposed to carbon ion irradiation. *Oncol Lett* 10: 2856-2864, 2015.
11. Di CX, Yang LN, Zhang H, An LZ, Zhang X, Ma XF, Sun C, Wang XH, Yang R, Wu ZH and Si J: Effects of carbon-ion beam or X-ray irradiation on anti-apoptosis Δ Np73 expression in HeLa cells. *Gene* 515: 208-213, 2013.
12. Conforti F, Yang AL, Agostini M, Rufini A, Tucci P, Nicklison-Chirou MV, Grespi F, Velletri T, Knight RA, Melino G and Sayan BS: Relative expression of TAp73 and Δ Np73 isoforms. *Aging (Albany NY)* 4: 202-205, 2012.
13. John K, Alla V, Meier C and Putzer BM: GRAMD4 mimics p53 and mediates the apoptotic function of p73 at mitochondria. *Cell Death Differ* 18: 874-886, 2011.
14. Muppani N, Nyman U and Joseph B: TAp73 α protects small cell lung carcinoma cells from caspase-2 induced mitochondrial mediated apoptotic cell death. *Oncotarget* 2: 1145-1154, 2011.
15. Bailey SG, Cragg MS and Townsend PA: Family friction as Δ Np73 antagonises p73 and p53. *Int J Biochem Cell Biol* 43: 482-486, 2011.
16. Di C, Sun C, Li H, Si J, Zhang H, Han L, Zhao Q, Liu Y, Liu B and Miao G, *et al*: Diallyl disulfide enhances carbon ion beams-induced apoptotic cell death in cervical cancer cells through regulating TAp73/ Δ Np73. *Cell Cycle* 14: 3725-3733, 2015.
17. Hassan HM, Dave BJ and Singh RK: TP73, an under-appreciated player in non-Hodgkin lymphoma pathogenesis and management. *Curr Mol Med* 14: 432-439, 2014.
18. Liu X, Sun C, Jin X, Li P, Ye F, Zhao T, Gong L and Li Q: Genistein enhances the radiosensitivity of breast cancer cells via G₂/M cell cycle arrest and apoptosis. *Molecules* 18: 13200-13217, 2013.
19. Cooper A, Garcia M, Petrovas C, Yamamoto T, Koup RA and Nabel GJ: HIV-1 causes CD4 cell death through DNA-dependent protein kinase during viral integration. *Nature* 498: 376-379, 2013.
20. Wang Y, Xue H, Cutz JC, Bayani J, Mawji NR, Chen WG, Goetz LJ, Hayward SW, Sadar MD, Gilks CB, *et al*: An orthotopic metastatic prostate cancer model in SCID mice via grafting of a transplantable human prostate tumor line. *Lab Invest* 85: 1392-1404, 2005.
21. Vandersickel V, Depuydt J, Van Bockstaele B, Perletti G, Philippe J, Thierens H and Vral A: Early increase of radiation-induced gammaH2AX foci in a human Ku70/80 knockdown cell line characterized by an enhanced radiosensitivity. *J Radiat Res* 51: 633-641, 2010.
22. Shiloh Y and Ziv Y: The ATM protein kinase: Regulating the cellular response to genotoxic stress and more. *Nat Rev Mol Cell Biol* 14: 197-210, 2013.
23. Yang J, Yu Y, Hamrick HE and Duerksen-Hughes PJ: ATM, ATR and DNA-PK: Initiators of the cellular genotoxic stress responses. *Carcinogenesis* 24: 1571-1580, 2003.
24. Durocher D and Jackson SP: DNA-PK, ATM and ATR as sensors of DNA damage: Variations on a theme? *Curr Opin Cell Biol* 13: 225-231, 2001.
25. Jackson SP: DNA damage detection by DNA dependent protein kinase and related enzymes. *Cancer Surv* 28: 261-279, 1996.
26. Yang C, Wang Q, Liu X, Cheng X, Jiang X, Zhang Y, Feng Z and Zhou P: NU7441 enhances the radiosensitivity of liver cancer cells. *Cell Physiol Biochem* 38: 1897-1905, 2016.
27. Tichy A, Durisova K, Salovska B, Pejchal J, Zarybnicka L, Vavrova J, Dye NA and Sinkorova Z: Radio-sensitization of human leukaemic MOLT-4 cells by DNA-dependent protein kinase inhibitor, NU7441. *Radiat Environ Biophys* 53: 83-92, 2014.
28. Niazi MT, Mok G, Heravi M, Lee L, Vuong T, Aloyz R, Panasci L and Muanza T: Effects of dna-dependent protein kinase inhibition by NU7026 on dna repair and cell survival in irradiated gastric cancer cell line N87. *Curr Oncol* 21: 91-96, 2014.
29. Chen H, Zeng X, Gao C, Ming P, Zhang J, Guo C, Zhou L, Lu Y, Wang L, Huang L, *et al*: A new arylbenzofuran derivative functions as an anti-tumour agent by inducing DNA damage and inhibiting PARP activity. *Sci Rep* 5: 10893, 2015.
30. Williamson CT, Muzik H, Turhan AG, Zamò A, O'Connor MJ, Bebb DG and Lees-Miller SP: ATM deficiency sensitizes mantle cell lymphoma cells to poly(ADP-ribose) polymerase-1 inhibitors. *Mol Cancer Ther* 9: 347-357, 2010.
31. Weston VJ, Oldreive CE, Skowronska A, Oscier DG, Pratt G, Dyer MJ, Smith G, Powell JE, Rudzki Z and Kearns P, *et al*: The PARP inhibitor olaparib induces significant killing of ATM-deficient lymphoid tumor cells in vitro and in vivo. *Blood* 116: 4578-4587, 2010.
32. Arlander SJ, Greene BT, Innes CL and Paules RS: DNA protein kinase-dependent G2 checkpoint revealed following knockdown of ataxia-telangiectasia mutated in human mammary epithelial cells. *Cancer Res* 68: 89-97, 2008.
33. Shen Y, Rehman FL, Feng Y, Boshuizen J, Bajrami I, Elliott R, Wang B, Lord CJ, Post LE and Ashworth A: BMN 673, a novel and highly potent PARP1/2 inhibitor for the treatment of human cancers with DNA repair deficiency. *Clin Cancer Res* 19: 5003-5015, 2013.
34. Sarkaria JN, Busby EC, Tibbetts RS, Roos P, Taya Y, Karnitz LM and Abraham RT: Inhibition of ATM and ATR kinase activities by the radiosensitizing agent, caffeine. *Cancer Res* 59: 4375-4382, 1999.
35. Rosenzweig KE, Youmell MB, Palayoor ST and Price BD: Radiosensitization of human tumor cells by the phosphatidylinositol3-kinase inhibitors wortmannin and LY294002 correlates with inhibition of DNA-dependent protein kinase and prolonged G2-M delay. *Clin Cancer Res* 3: 1149-1156, 1997.
36. Critchlow SE, Bowater RP and Jackson SP: Mammalian DNA double-strand break repair protein XRCC4 interacts with DNA ligase IV. *Curr Biol* 7: 588-598, 1997.
37. Davidson D, Amrein L, Panasci L and Aloyz R: Small molecules, inhibitors of DNA-PK, targeting DNA repair and beyond. *Front Pharmacol* 4: 5, 2013.
38. Blasina A, Hallin J, Chen E, Arango ME, Kraynov E, Register J, Grant S, Ninkovic S, Chen P, Nichols T, *et al*: Breaching the DNA damage checkpoint via PF-00477736, a novel small-molecule inhibitor of checkpoint kinase 1. *Mol Cancer Ther* 7: 2394-2404, 2008.
39. Sausville EA, Arbuck SG, Messmann R, Headlee D, Bauer KS, Lush RM, Murgo A, Figg WD, Lahusen T, Jaken S, *et al*: Phase I trial of 72-hour continuous infusion UCN-01 in patients with refractory neoplasms. *J Clin Oncol* 19: 2319-2333, 2001.



This work is licensed under a Creative Commons Attribution-NonCommercial-NoDerivatives 4.0 International (CC BY-NC-ND 4.0) License.